Original Article

Check for updates

Protective Effects of *Changbudodam-tang* on Cell Death Signals on the Bone Marrow-Derived Human Mesenchymal Stem Cells via Regulation of MKK7/JNK/c-Jun Signaling Pathway

Hee-Jae Yoon[1], Si-Yoon Cho[1], Hyeong-Geug Kim[2], Ji-Yeon Lee[1]*

[1]Department of Obstetrics and Gynecology, College of Korean Medicine, Daejeon University, Daejeon, Republic of Korea
[2]Department of Leukopak Research and Developement, QPS Bio-Kinetic, Springfield, MO, USA

*Corresponding Author
Ji-Yeon Lee
Department of Obstetrics and Gynecology, College of Korean Medicine, Daejeon University, 62 Daehak-ro, Dong-gu, Daejeon 34520, Republic of Korea
Tel: +82-42-470-9139
E-mail: jyounl@daum.net

Objectives: Polycystic ovary syndrome (PCOS) is one of the most common disorders and it shows up to 20% prevalence in reproductive-aged women populations, but no cures are available to date. We aimed to investigate the protective effects of *Changbudodam-tang* (CBD) on cell death signaling pathways, inflammation, and oxidative stress observed in Bone-Marrow derived human mesenchymal stem cell (BM-hMSC) by means of PCOS therapeutics in the future.
Methods: BM-hMSCs were applied with cell deaths and injuries. Apoptosis and pyroptosis signals were quenched with their related signaling pathways using quantitative PCR, Western blot, and fluorescence image analysis.
Results: Our data clearly displayed hydrogen peroxide- and nigericin-treated cell death signaling pathways via regulations of mitochondrial integrity and interleukin (IL)-1β at the cellular levels ($p < 0.01$ or 0.001). We further observed that pre-treatment with CBD showed protective effects against oxidative stress by enhancement of antioxidant components at the cellular level, with respect to both protein and mRNA expression levels ($p < 0.05$, 0.01 or 0.001). The mechanisms of CBD were examined by Western blot analysis, and it showed anti-cell death, anti-inflammatory, and antioxidant effects via normalizations of the Jun N-terminal kinase/mitogen-activated protein kinase kinase 7/c-Jun signaling pathways.
Conclusion: This study confirmed the pharmacological properties of CBD by regulation of cellular oxidation and the inflammation-provoked cell death condition of BM-hMSCs, which is mediated by the MKK7/JNK/c-Jun signaling pathway.

Keywords: *changbudodam-tang* (CBD), polycystic ovary syndrome (PCOS), apoptosis, pyroptosis, oxidative stress

INTRODUCTION

Polycystic ovary syndrome (PCOS) is one of the most common disorders among women of reproductive age, affecting approximately 20% of this population [1]. PCOS leads to various symptoms including hyperandrogenism, ovulatory dysfunction, and polycystic ovarian morphological alterations [2, 3]. The pathophysiological mechanism of PCOS remains to be elucidated. Previous studies have reported that complex endocrine dysfunctions and metabolic syndrome mainly contribute to PCOS [4]. These conditions aggravate low to mild chronic inflammation and oxidative stress, contributing to the progression and development of PCOS. Here, the release of pro-inflammatory cytokines leads to an abnormal increase in androgen generation in theca cells [5, 6]. Furthermore, the excessive generation of reactive oxygen species (ROS) exerts oxidative stress by ac-

tivating ROS-sensitive pathways, such as the c-Jun N-terminal kinases (JNK) signaling pathways [7]. Thus, a combination of anti-inflammatory and antioxidant treatments may be a potent therapeutic strategy for treating patients with PCOS.

Recently, physicians have been recommending lifestyle changes to patients for managing PCOS and metabolic syndrome-related disorders. These changes include a healthy diet, weight loss, and increased physical activity. Another way to manage these disorders may be to take health supplements with antioxidant effects (Ref). In addition, previous studies have reported the utilization of bone marrow human mesenchymal stem cells (BM-hMSC) for enhanced anti-inflammatory effects with immunosuppression in animal models [8, 9].

According to Traditional Oriental Medicine (TOM), herbal medicines and acupuncture treatments are also effective in managing PCOS [10, 11]. Specifically, *Changbudodam-tang* (CBD) has been traditionally and widely used in the clinic to ameliorate patients' PCOS symptoms [12-14]. However, the potential anti-inflammatory actions of CBD remain elusive.

In this study, we aimed to investigate the pharmacological effects of CBD on BM-hMSCs under various cell-damaging stimuli, such as cell death signals, inflammatory conditions, and oxidative stress. The potential molecular signaling pathways associated with CBD's anti-inflammatory and anti-cell injury effects were investigated.

MATERIALS AND METHODS

1. Preparation of *Changbudodam-Tang* (CBD)

CBD, composed of a total of six types of herbal medicines, was prepared by Daeyeon Pharmaceutical (Incheon, South Korea). The preparation was done in a clean room, following the good manufacturing practices (GMP) approved by the Ministry of Food and Drug Safety (MFDS). The ingredients of CBD and their ratios are listed in Table 1. A total of 54 g of dry CBD ingredients were washed twice using distilled water (DW). The ingredients were then incubated in a dry oven overnight at 60℃ for complete drying needed for extraction. Next, the ingredients were boiled for 3 hours, concentrated for 1.5 hours, and frozen at –80℃ for lyophilization. The resulting CBD powder was then dissolved in DW and centrifuged. The supernatant (20 mg/mL) was filtered using a 0.45 µm syringe applied filter (Millipore) and stored at –80℃ until usage.

Table 1. Ingredients and ratios of *Changbudodam-tang* (CBD)

Herbal name	Specific name origin	Amount (g)
Atractylodis Rhizom	Atractylodes lancea De Candlle (Vietnam)	12
Cyperi Rhizoma	Cyperus rotundus Linné (Korea)	12
Aurantii Fructus Immatur	Citrus aurantium Linné (China)	12
Citri Unshius Pericarpiu	Citrus reticulata Blanc (Korea)	6
Astragali Radix	Astragalus membranaceus Bunge (China)	6
Cinnamomi Cortex	Cinnamomum cassia Presl (Vietnam)	6
Total		54

2. Cell culture

BM-hMSCs were kindly provided by Dr. Chang-Hyun Gil in the Department of Surgery at Indiana University School of Medicine. The cells were cultured in Xeno-Free BM-hMSC Expansion Media (Sartorius, Goettingen, Germany) supplemented with 10% fetal bovine serum (FBS; Sigma Aldrich, MO, USA). The cells were seeded in culture dishes of either 60 mm or 35 mm diameter depending on the experiment.

3. Induction of cell death in BM-hMSCs

To investigate the protective effects of CBD against cell death signals, BM-hMSCs were first treated with 200 or 400 µg/mL CBD or 2 ng/mL human transformation growth factor (TGF)-β1 for 6 hours. Next, the cells were treated with hydrogen peroxide, nigericin, or TNF-α. Upon completion of each treatment, the medium was removed and the cells were washed twice with 10 mM phosphate-buffered saline (PBS). Next, the cells were harvested using 0.5% Tris-ethylenediaminetetraacetic acid (EDTA; Invitrogen) and subjected to appropriate experimental procedures for testing.

4. LIVE/DEAD cell assay

BM-hMSCs were seeded in a 35-mm diameter glass bottom dish at 1×10^5 cells/dish. After reaching 60-70% confluence, the cells were treated with the media containing CBD or TGF-β1 for 6 hrs. Next, the cells were treated with 500 µM hydrogen peroxide for 24 hours. The cells were then rinsed twice with PBS and treated with the LIVE/DEAD cell reagents (Invitrogen™, Cat#. L3224) according to the manufacturer's protocol.

The cells were imaged at 200× magnification using an LSM 700 confocal microscope (Carl Zeiss AG, Oberkochen, Baden-Wurttemberg, Germany); green fluorescence indicated live cells and red fluorescence indicated dead cells. The captured images were analyzed using Image J version 1.64 (National Institute of Health, MD, USA).

5. Flow cytometry

Flow cytometry (fluorescence assisted cell sorting or FACS, BD Biosciences, NJ, USA) was used to analyze the levels of apoptosis (Annexin V and PI), pyroptosis (PI), cleaved caspase-1 (p10), and interleukin (IL)-1β in the treated cells. For the apoptosis assay, the cells were initially treated with CBD or TGF-β1 for 6 hours, followed by 500 μM hydrogen peroxide treatment for 12 hours. The cells were harvested and stained with PI/Annexin V following the manufacturer's protocol (Cat#. 88-8005-74, Thermo Fisher). For the pyroptosis assay, the cells were identically treated with CBD or TGF-β1, followed by 3 μM nigericin (3 μM) treatment for 12 hours. The cells were analyzed using a pyroptosis detection kit (Cat#. SKU. 9145, Immunohistochemistry Technology, CA, USA) following the

manufacturer's protocol. For the IL-1β assay, the cells were identically treated with CBD or TGF-β1 and nigericin. The cells were then treated with a permeabilization buffer (0.1% Triton X) for 10 minutes at room temperature (RT), followed by incubation with IL-1β antibody (10 μM Human IL-1 beta/IL-1F2 APC-conjugated antibody, Cat#. IC8406A, R&D Systems, MN, USA).

6. Real-time reverse transcription polymerase chain reaction (RT-PCR) analysis

First, mRNA was isolated from the treated cells using the TRIZOL Reagent (Sigma-Aldrich). cDNA was synthesized with 1 μg of the isolated mRNA using a commercial kit. Real-time RT-PCR was performed using the synthesized cDNA and SYBR Green qPCR kit (Cat#. 4368814, Applied Biosystems™). The PCR reactions were conducted using Mastercycler RealPlex 2 (Eppendorf, Hauppauge, NY, USA) with a total of 10 μL of final reaction volume (5 μL of SYBR Green Supermix, 2 μL RNase free water, 1 μL of 10 pM primer pairs, and 2 μL of cDNA) (Table 2). The PCR reaction conditions were as follows: 2 minutes at 50℃ for uracil-DNA glycosylase (UDG) activation, 2 min-

Table 2. Primer list for real-time PCR

Gene	Species	Primer sequence (forward and reverse)	Application
TNFA	Human	5′- CTC TTC TGC CTG CTG CAC TTT G-3′ 5′- ATG GGC TAC AGG CTT GTC ACT C-3′	qPCR
IL1B	Human	5′- CCA CAG ACC TTC CAG GAG AAT G-3′ 5′- GTG CAG TTC AGT GAT CGT ACA GG-3′	qPCR
IL10	Human	5′- TCT CCG AGA TGC CTT CAG CAG A-3′ 5′- TCA GAC AAG GCT TGG CAA CCC A-3′	qPCR
GSS	Human	5′-TAT GTG AGC CGC CTG AAT GCC A-3′ 5′-TGT GAC CTC TCC AGC AGT AGA C-3′	qPCR
GPX3	Human	5′-TAC GGA GCC CTC ACC ATT GAT G-3′ 5′-CAC TGA CCT CTA TTG TGG GCT TG-3′	qPCR
GRS	Human	5′-GTT TAC CGC TCC ACA CAT CCT G-3′ 5′-GCT GAA AGA AGC CAT CAC TGG TG-3′	qPCR
CAT	Human	5′- GTG CGG AGA TTC AAC ACT GCC A-3′ 5′- CGG CAA TGT TCT CAC ACA GAC G-3′	qPCR
SOD1	Human	5′-CTC ACT CTC AGG AGA CCA TTG C-3′ 5′-CCA CAA GCC AAA CGA CTT CCA G-3′	qPCR
SOD2	Human	5′-CTG GAC AAA CCT CAG CCC TAA C-3′ 5′-AAC CTG AGC CTT GGA CAC CAA C-3	qPCR
SOD3	Human	5′-CAC CAT TGG CAA TGA GCG GTT C-3′ 5′-TGG CTG ATG GTT GTA CCC TGC A-3′	qPCR
β-ACTIN	Human	5′-GGC ACC ACA CCT TCT ACA ATG A-3′ 5′-AGG TCT TTG CGG ATG TCC ACG T-3′	qPCR

utes at 95℃ for DNA polymerase, and 40 cycles of amplification steps (15 seconds at 95℃, 15 seconds at 60℃, and 15 seconds at 72℃). The mRNA expression levels were analyzed using β-actin as the housekeeping gene and calculated by $2^{-\Delta\Delta CT}$.

7. Protein sample preparation

The treated cells were harvested and treated with radio-immunoprecipitation assay (RIPA) buffer containing cocktail proteinase inhibitors and phosphorylated inhibitors (Cat#. ab201119, Abcam). The lysate was centrifuged at $12,000 \times g$ at 4℃ for 60 minutes. The protein concentration in the supernatant was measured via BCA assay (Compat-Able™ BCA Protein Assay Kit, Cat#. 23229, Thermo Fisher).

8. Protein levels of pro- and anti-inflammatory cytokines in the liver

Enzyme-linked immunosorbent assay kits were used to determine the protein levels of pro- and anti-inflammatory cytokines (BD Biosciences for TNF-α and IL-6 ELSIA; R&D Systems for IL-1β and IL-10 ELISA).

9. Mitochondria integrity

Mitochondrial integrity was analyzed using MitoTracker (Cat#. M7512, MitoTracker™ Red CMXRos, Invitorgen™). The deep red fluorescence signals were analyzed using a confocal microscope at 200× magnification.

10. Biochemical assays

The cells were seeded in either a glass-bottom dish of 35 mm diameter or a 96-well microplate at 1×10^5 cells/well and 2×10^3 cells/well, respectively. After treating the cells with either the drug or hydrogen peroxide, 10 μL of 1 μM dichlorodihydrofluorescein diacetate (DCFDA; Cat#. D399, Invitrogen™) was added and incubated for 30 minutes at 37℃ in the dark.

The presence of ROS was imaged by green fluorescence under a confocal microscope at 200× magnification. For the quantification of ROS level, the cells were lysed with 2N HCl and subjected to UV-Vis spectroscopy (excitation at 488 nm and emission at 535 nm). The lipid peroxidation level was also determined based on the malondialdehyde (MDA) concentration using a commercial kit (Cat#. K739, Bio Vision).

The total thiol level was measured by staining with a fluorescent probe (Cat#. T10096, ThiolTracker™, Invitrogen™) and imaging with a confocal microscope. The total glutathione (GSH) content, SOD activity, and catalase activity in the cell lysates were measured using commercial kits (GSH kit: Cat#. EIAGSHC, Invitrogen; SOD activity kit: Cat#. 19160, Millipore Sigma; Catalase activity kit: EIACATC, Thermo Fisher). A plate reader (Versa Max, SoftMax 5.14) was used for these analyses.

11. Western blot

The protein samples were separated on an SDS-PAGE gel and transferred to a PVDF membrane (Millipore, Billerica, Massachusetts, USA). The membrane was incubated in 5% skim milk (in 0.05% PBST buffer) for 1 hour to block non-specific protein binding. The membrane was then incubated with the following primary antibodies: anti-rabbit-MKK7 antibody (CST, #4172), anti-rabbit-phosphorylated MKK7 (Ser271/Thr275) antibody (CST, #4171), anti-rabbit-SAPK/JNK antibody (CST, #9252), anti-rabbit phosphorylated SAPK/JNK (Thr183/Tyr185) (81E11) antibody (CST, #4668), anti-rabbit-c-Jun antibody (CST, #9165), and anti-rabbit-phosphorylated-c-Jun (Ser73)(D47G9)XP® antibody (CST, #3270). Anti-mouse-α-actinin (SCBT, sc-17829, 1:3000) was used as the inner control. After incubating overnight at 4℃, the blots were rinsed thrice with PBST buffer. The blots were then incubated with horseradish peroxidase (HRP)-conjugated secondary antibodies and washed with PBST buffer. The blots were visualized using a chemiluminescent detection reagent (Thermo Fisher Scientific).

12. Statistical analysis

All values were expressed as mean ± standard error of the mean (SEM). The statistical significances of the differences among the groups were analyzed by one-way ANOVA followed by post-hoc multiple comparisons with Tukey t-test using Prism version 9.3.1 (GraphPad 10.01, California, USA). A p-value of less than 0.05 was considered statistically significant.

RESULTS

1. Anti-apoptotic effects of CBD

We first confirmed CBD's impact on cell viability via LIVE/

DEAD cell analysis. As shown in Fig. 1A and B, H_2O_2 treatment significantly increased the signals corresponding to dead cells (red fluorescence) compared to the control group ($p < 0.001$). Furthermore, H_2O_2 treatment also deteriorated the cells' mitochondrial integrity as shown by the significantly diminished signals (red fluorescence) ($p < 0.001$ in Fig. 1C, D). These cellular damages were significantly protected by the pre-treated CBD, particularly at 400 μg/mL ($p < 0.001$ for 400 μg/mL CBD in Fig. 1B and $p < 0.001$ for both 200 and 400 μg/mL CBD in Fig. 1D).

Flow cytometry indicated that CBD showed a potent anti-apoptotic effect under H_2O_2-induced stress, as shown by the decreased cell populations in the double-positive quadrant areas corresponding to Annexin V- and PI-stained cells compared to the H_2O_2-only group ($p < 0.01$ or 0.001 in Fig. 1E, F).

The treatment of human recombinant TGF-β1, which was used as the positive control, also showed protective effects against H_2O_2-induced stress compared to the H_2O_2-only group, as demonstrated by LIVE/DEAD cell analysis, mitochondrial integrity, and Annexin V assay ($p < 0.01$ or 0.001 in Fig. 1).

2. Anti-pyroptotic effects of CBD

We next examined the protective effects of CBD against pyroptosis, which was induced with nigericin. As expected, the hMSC population in the double-positive area of PI and cleaved caspase-1 (p10) was significantly increased in the nigericin-treated group compared to the control group ($p < 0.001$ in Fig. 2A, B), indicating the induction of pyroptosis. Pre-treatment of the cells with CBD significantly inhibited pyroptosis, as demonstrated by flow cytometry analysis ($p < 0.01$ for 200 μg/mL CBD and $p < 0.001$ for 400 μg/mL CBD in Fig. 2A, B).

As a result of the elevated level of pyroptosis, the cell population in the IL-1β/F2-positive area was significantly increased in the nigericin-treated group compared to the control group ($p < 0.001$ in Fig. 2C, D). Such elevation of pyroptosis could be significantly inhibited by pre-treating the cells with CBD ($p < 0.01$ for 200 μg/mL CBD and $p < 0.001$ for 400 μg/mL CBD in Fig. 2C, D). Both the mRNA and protein levels of IL-1β well supported the observed pyroptosis induced by nigericin treatment ($p < 0.001$ for both the mRNA and protein expression levels in
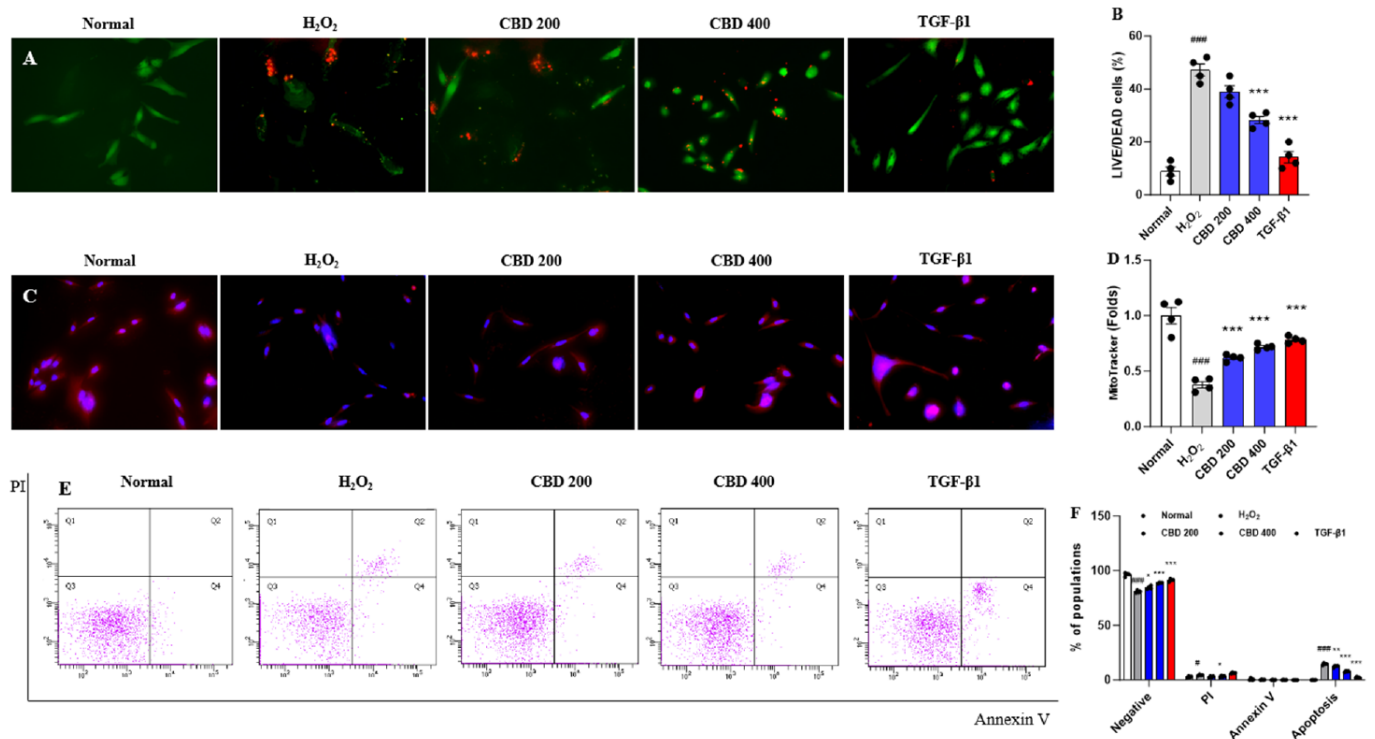
Figure 1. Protective effects of the CBD on the apoptosis signals. (A) Fluorescence analysis of the LIVE/DEAD and (B) its quantification. (C) Fluorescence image analysis of Mitochondrial integrity and (D) its quantification analysis. (E) Flow cytometry analysis of apoptosis using Annexin V and (F) its quantification analysis. Images were captured by a fluorescence filter equipped with microscopy conditions (200- and 400- ×). Data are expressed as mean ± S.E.M (n = 4 to 6 for each group). ##p < 0.01 and ###p < 0.001 vs. normal group; *p < 0.05, **p < 0.01 and ***p < 0.001 vs. H_2O_2 group.
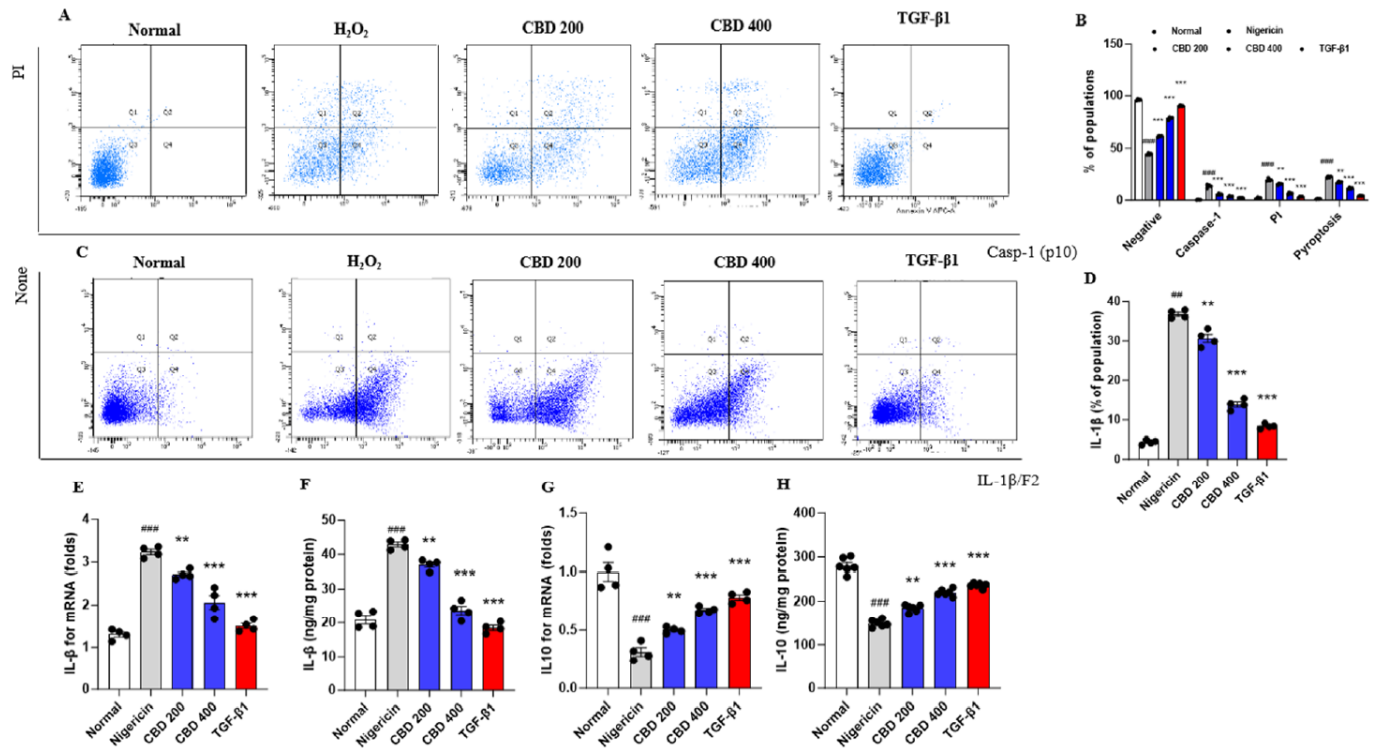
Figure 2. Protective effects of the CBD on the Pyroptosis signals and increases of IL-10. (A) Flow cytometry analysis of Pyroptosis and (B) its quantification analysis. (C) Flow cytometry analysis of IL-1β/F2 and (D) its quantification analysis. (E) mRNA expression levels of IL-1β and (F) protein levels of IL-1β/F2. (G) mRNA expression levels of IL-10 and (H) protein levels of IL-10. Data are expressed as mean ± S.E.M (n = 4 to 6 for each group). ##p < 0.01 and ###p < 0.001 vs. normal group; **p < 0.01 and ***p < 0.001 vs. H₂O₂ group.

Fig. 2E, F), as well as the protective effects of CBD (p < 0.01 for 200 μg/mL CBD and p < 0.001 for 400 μg/mL CBD in Fig. 2E, F). The mRNA and protein levels of IL-10, an anti-inflammatory cytokine, were significantly decreased in the nigericin-treated group compared to the control group (p < 0.001 in Fig. 2G, H). Pre-treating the cells with CBD inhibited such reduction in IL-10 (p < 0.001 in Fig. 2G, H).

The positive control group (TGF-β1) showed a potent protective effect against nigericin-induced pyroptosis as demonstrated by flow cytometry, as well as the mRNA and protein expression levels (p < 0.001 in Fig. 2).

3. CBD's protective effects against cellular oxidative stress

To further investigate the protective effects of CBD against apoptosis and pyroptosis, we assessed CBD's antioxidant effects. Cellular oxidative stress in hMSCs was significantly induced in the cells treated with H₂O₂, as demonstrated by staining with DCFDA (intracellular H₂O₂; green fluorescence) and DHE (superoxide radicals; red fluorescence), compared to the control

group (p < 0.001 for DCFDA in Fig. 3A, B; p < 0.01 for DHE in Fig. 3C, D). Pre-treatment with CBD significantly reduced such abnormal increase in ROS induced by H₂O₂ treatment (p < 0.01 for 200 μg/mL CBD and p < 0.001 for 400 μg/mL CBD for both DCFDA and DHE shown in Fig. 3A-D).

The intracellular level of H₂O₂ was significantly increased in the H₂O₂-treated group compared to the control group (p < 0.001 in Fig. 3E). Furthermore, the level of lipid peroxidation, which is the final product of oxidative stress, was also significantly increased in the H₂O₂-treated group compared to the control group, as demonstrated by MDA measurements (p < 0.001 in Fig. 3F). Pre-treatment with CBD significantly reduced such oxidative damage to the cells (p < 0.01 for 200 μg/mL CBD and p < 0.001 for 400 μg/mL CBD for ROS and MDA shown in Fig. 3E, F).

Human recombinant TGF-β1 treatment significantly decreased all oxidative stress mediators and MDA compared to the H₂O₂-treated group (p < 0.001 for all parameters shown in Fig. 3).
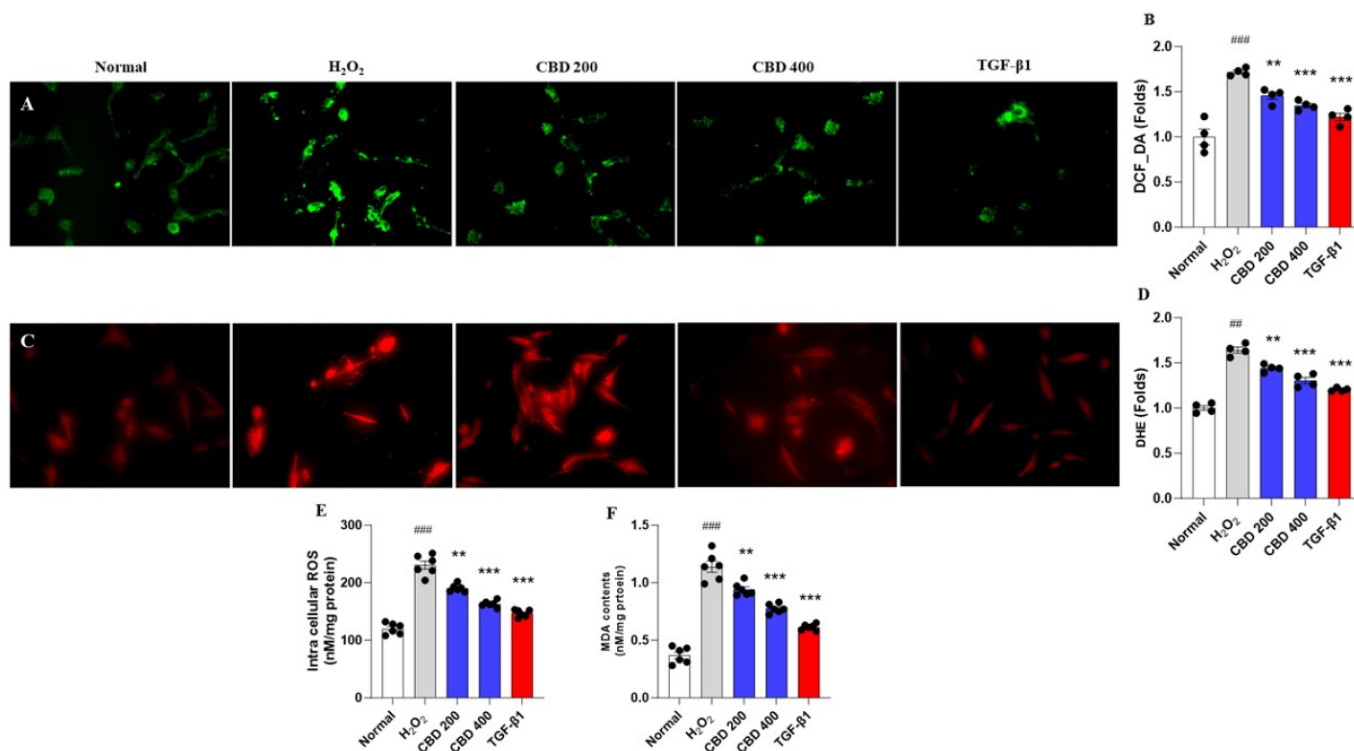
Figure 3. Protective effects of CBD on cellular oxidative stress. (A) Fluorescence images for the detection of DCF_DA and (B) quantification. (C) Detection of DHE using fluorescence images and (D) quantification analysis. (E) Intracellular ROS levels and (F) MDA contents from protein lysates. Images were captured by a fluorescence filter equipped with microscopy conditions (200×). Data are expressed as mean ± S.E.M (n = 4 to 6 for each group). ##$p < 0.01$ and ###$p < 0.001$ vs. normal group; **$p < 0.01$ and ***$p < 0.001$ vs. H_2O_2 group.
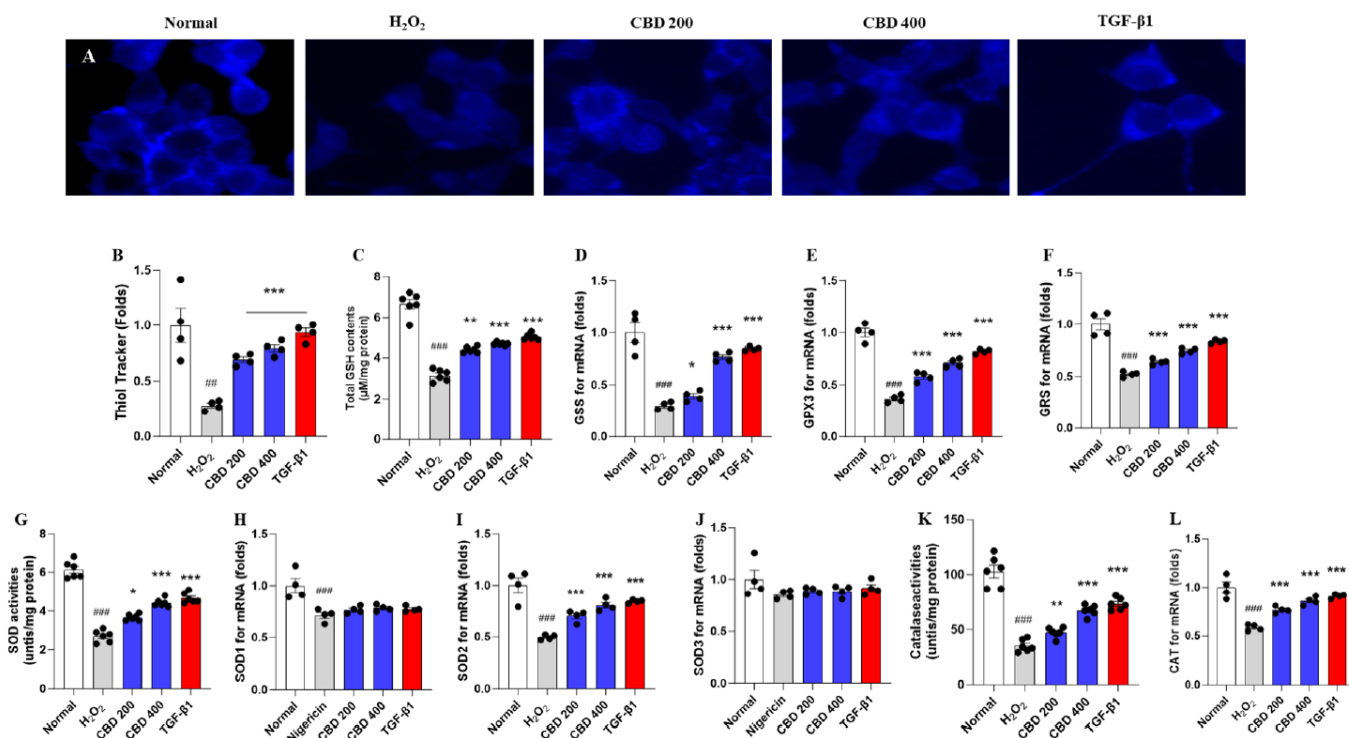
4. Antioxidant effects of CBD

We further assessed the pharmacological effects of CBD, with a focus on its antioxidant components. The fluorescence imaging analysis indicated that the presence of thiols, which are present in GSH, was significantly decreased upon H_2O_2 treatment compared to the control group ($p < 0.01$ in Fig. 4A, B). Pre-treatment with CDB significantly prevented such depletion of thiols observed in the H_2O_2-treated group ($p < 0.001$ for both 200 and 400 µg/mL CBD shown in Fig. 4A, B).

The protein level of total GSH content was also significantly decreased by H_2O_2 treatment ($p < 0.001$ in Fig. 4C). Pre-treatment with CBD, again, significantly reduced the depletion of GSH compared to the H_2O_2-treated group ($p < 0.01$ for 200 µg/mL CBD and $p < 0.001$ for 400 µg/mL CBD shown in Fig. 4C). The mRNA levels of GSH-related enzymes, such as GSS, GPX3, and GRS, significantly decreased in the H_2O_2-treated group by 0.35-, 0.41-, and 0.50-fold compared to the control group ($p < 0.001$ for all enzymes shown in Fig. 4D, F). Pre-treatment with CBD significantly normalized such abnormal gene expression levels

($p < 0.05$ for 200 µg/mL CBD in GSS; $p < 0.001$ for others in GSS, GRS, and GPX shown in Fig. 4D-F).

Enzymatic antioxidant components, SOD and catalase, also considerably decreased upon H_2O_2 treatment. The protein level of SOD significantly decreased in the H_2O_2-treated group compared to the control group ($p < 0.001$ in Fig. 4G). The gene expression levels of SOD family members, including SOD1 and SOD2, also significantly decreased in the H_2O_2-treated group by approximately 0.72-, 0.43-, and 0.87-fold compared to the control group ($p < 0.001$ for all members shown in Fig. 4H, I). However, the SOD3 level was not significantly altered ($p > 0.05$ in Fig. 4J). Respective reductions in SOD levels were significantly recovered by pre-treatment with CDB; SOD activities at the protein level and SOD2 at the mRNA level ($p < 0.001$ for SOD activities and mRNA level of SOD2 shown in Fig. 4G, I). However, SOD1 was not significantly altered ($p > 0.05$ in Fig. 4H).

The protein level of catalase, an antioxidant enzyme, was significantly decreased in the H_2O_2-treated group compared to the control group ($p < 0.001$ in Fig. 4K). The enzyme's gene ex-

Figure 4. Antioxidant effects of the CBD. (A) Fluorescence images for Thiol tracker and (B) quantification analysis. (C) Total GSH contents in the protein lysates of hMSCs. (D) mRNA expression levels of GSH systems including GSS, (E) GPX3, and (F) GRS. (G) SOD activities in the protein lysates of hMSCs and mRNA expression levels of SOD family members including (H) SOD1, (I) SOD2, and (J) SOD3. (K) Catalase activities in the protein lysates for hMSCs and (L) mRNA expression levels of CAT. Images were captured by fluorescence filters equipped with microscopy conditions (630×). Data are expressed as mean ± S.E.M (n = 4 to 6 for each group). $^{\#\#}p < 0.01$ and $^{\#\#\#}p < 0.001$ vs. normal group; $^{*}p < 0.05$, $^{**}p < 0.01$ and $^{***}p < 0.001$ vs. H_2O_2 group.

pression levels also decreased by 0.54-fold in the H_2O_2-treated group (p < 0.001 in Fig. 4L). These abnormal alterations were significantly normalized by pre-treatment with CBD (p < 0.01 for 200 μg/mL CBD for catalase activities in Fig. 4K; p < 0.001 for all others in Fig. 4K, L).

The positive control group, TGF-β1, showed strong antioxidant effects with statistically significant differences compared to the H_2O_2-treated group (p < 0.001 in Fig. 4A-G, I, K, L). However, the mRNA levels of SOD1 and SOD3 were not significantly affected by the treatment (Fig. 4H, J).

5. CBD exerts anti-cell death and antioxidant effects through JNK/MKK7/c-Jun signaling pathways

To examine the underlying mechanisms of CBD's pharmacological effects on cell death and oxidative stress, we carried out a western blot analysis focusing on the JNK/MKK7/c-Jun signaling pathways. As expected, the protein level of p-JNK was drastically increased by H_2O_2 treatment compared to the

control group. The downstream oxidative stress-induced cell injury and death signaling proteins, such as MKK7 and c-Jun, were also considerably enhanced in the H_2O_2-treated group. Remarkably, pre-treatment with CBD prevented such phenomena (Fig. 5A). Human recombinant TGF-β1 treatment also showed similar preventive effects (Fig. 5A).

DISCUSSION

BM-hMSC-based therapy is promising for managing PCOS, as this cell type exhibits self-renewing, proliferation, differentiation, and immunomodulatory activities under inflammatory conditions. BM-hMSCs are also highly associated with enhanced ovarian functions by regulating the paracrine signaling pathways. Additionally, the pathological features of PCOS are closely linked to inflammation and oxidative stress. These pathological conditions eventually lead to the activation of cell death signaling pathways. It has been demonstrated that BM-hMSC infusion can reduce inflammation in animals with letro-
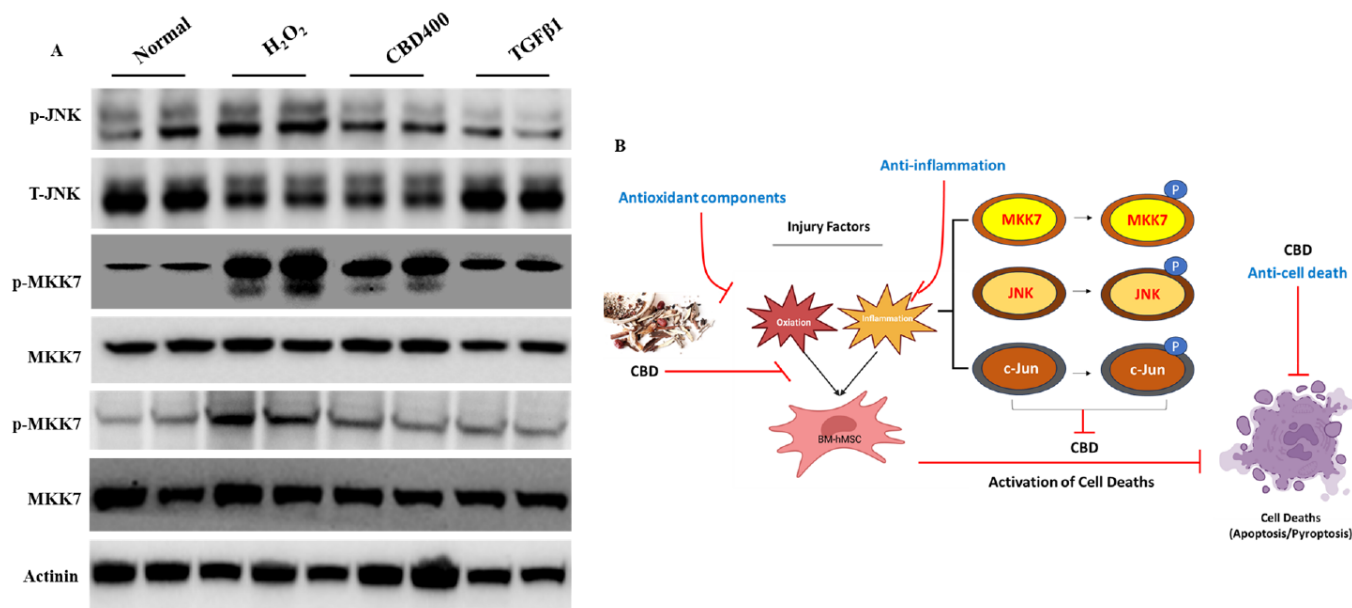
Figure 5. Western blot analysis of JNK, MKK7, and c-Jun signaling pathways and brief chart model of underlying mechanisms of the CBD on cell death and oxidative stress of hMSC. (A) Western blot analysis of p-JNK, JNK, p-MKK7, MKK7, p-c-Jun and c-Jun were performed using hMSC protein lysates. Actinin was used as inner control of the Western blot analysis. (B) Brief chart of pharmacological actions of the CBD via regulation of JNK/MKK7/c-Jun signaling pathway.

zole (LTZ)-induced PCOS [15, 16]. Based on previous studies, we hypothesized that BM-hMSCs combined with CBD may exhibit enhanced anti-inflammatory and antioxidant activities, thereby preventing the cell death signaling pathways with minimal stimuli.

In line with our expectation, we confirmed that CBD could efficiently inhibit cell death signals, particularly the H_2O_2-induced apoptosis and nigericin-induced pyroptosis signaling pathways (Figs. 1A, B, E, F, 2A, B). Regarding the protective effects of CBD, the mitochondrial integrity was associated with apoptosis (Fig. 1C, D), while pyroptosis was closely linked to IL-1β, with increases in both the gene and protein levels of IL-10 (Fig. 2C to H). H_2O_2 is a commonly used chemical for inducing cell death signals in MSCs [17]. Mitochondrial integrity is a critical factor in maintaining cell survival and respiration in biological organisms. When this integrity is altered, it directly leads to the activation of cell death signals, such as caspase signaling pathways and cytochrome c release [18, 19]. Pyroptosis, an inflammation-mediated cell death signaling pathway, is crucial for understanding the relationship between various types of cell death singling and inflammation (particularly the inflammasome signaling pathway) [20, 21]. As a crucial inflammatory cytokine, IL-1β directly mediates pyroptosis under specific conditions [20, 22].

Oxidative stress causes chronic inflammation and is one of the main pathological sources of PCOS [23, 24]. The antioxidant effects of CBD were confirmed by assessing the altered ROS levels via DCFDA and DHE staining (Fig. 3A-D). The decreased intracellular levels of ROS and MDA, the final product of oxidative stress, confirmed the antioxidant effects of CBD (Fig. 3F-G). ROS are harmful free radicals that directly damage the cells and DNA membranes [25]. We suspect that BM-hMSCs' potent antioxidant activities and culture with CBD may be improving redox homeostasis [26]. Antioxidants are equipped with non-enzymatic and enzymatic components for protection against oxidative damage. GSH is a peptide that quenches free radical adducts through the regulation of its related enzymes [27]. Enzymatic antioxidant components, such as SOD and catalase, play critical roles in preventing severe oxidative stress by removing ROS during cellular oxidation [27, 28]. SOD is an enzyme that converts superoxide to hydrogen peroxide, which is catalyzed by catalase activities. These properties were well demonstrated in BM-hMSCs' redox status at both the protein and gene levels (Fig. 4A-L).

To investigate the pharmacological actions of CBD against cell death signals, inflammation, and oxidative stress, we performed a western blot analysis focusing on the JNK/MKK7/c-Jun signaling pathways. The cell death signaling pathway result-

ing from oxidative stress and inflammation is mediated by the MKK7/JNK/c-Jun-singling pathway [29]. In MSCs, JNK plays a critical role in cell differentiation and renewal by cooperating with MKK7 [30]. c-Jun is responsible for osteogenic and adipogenic differentiation in MSCs [31]. However, there is no evidence to explain cell death by cellular oxidation and inflammation.

In this study, the protein level of MKK7 was enhanced by hydrogen peroxide treatment. The phosphorylated JNK and the MKK7/JNK signaling pathway mediate c-Jun activation through phosphorylation, which is a major cell death factor [32]. Pre-treatment with CBD significantly prevented this effect compared to the H_2O_2-treated group (Fig. 5A).

Despite the high morbidity of PCOS among reproductive women, there is no off-the-shelf drug available. However, the application of MSCs has shown promising potential as an effective treatment option for PCOS. In this study, we examined the therapeutic effects of CBD which is a modified prescription of TOM. The uses of herbal materials are accompanied by several critical issues, such as contamination, original sources, and chemical characterization (Advancing herbal medicine: enhancing product quality and safety through robust quality control practices). To minimize these issues, we used a GMP facility supplied with clearly defined raw materials.

For facile production and material preparation, further studies are needed to elucidate the effects and actions of CBD using pre-clinical animal models. This will involve administering CBD directly and using MSCs pre-cultured with CBD. Furthermore, the MKK/JNK/c-Jun signaling pathways will need to be explored.

CONCLUSION

We explored the potential of BM-hMSC for treating PCOS through anti-inflammatory and antioxidant effects. These effects were associated with various anti-cell death effects. CBD showed potent inhibitory effects against apoptosis and pyroptosis, which are mainly mediated by inflammation and oxidative stress at the cellular level. The underlying mechanisms may be associated with both the inflammation- and oxidation-related signaling pathways, particularly the MKK7/JNK/c-Jun signaling pathway (Fig. 5B).

ORCID

Hee-Jae Yoon, https://orcid.org/0000-0002-5102-1317
Si-Yoon Cho, https://orcid.org/0000-0002-3688-8799
Hyeong-Geug Kim, https://orcid.org/0000-0002-1473-6620
Ji-Yeon Lee, https://orcid.org/0000-0002-2140-2581

REFERENCES

1. Fauser BC, Tarlatzis BC, Rebar RW, Legro RS, Balen AH, Lobo R, et al. Consensus on women's health aspects of polycystic ovary syndrome (PCOS): the Amsterdam ESHRE/ASRM-Sponsored 3rd PCOS Consensus Workshop Group. Fertil Steril. 2012;97(1):28-38.e25.

2. Clapp C, de la Escalera GM. Peripheral regulation of prolactin by oxytocin: focus on "systemic oxytocin induces a prolactin secretory rhythm via the pelvic nerve in ovariectomized rats". Am J Physiol Regul Integr Comp Physiol. 2011;301(3):R674-5.

3. Helena CV, Cristancho-Gordo R, Gonzalez-Iglesias AE, Tabak J, Bertram R, Freeman ME. Systemic oxytocin induces a prolactin secretory rhythm via the pelvic nerve in ovariectomized rats. Am J Physiol Regul Integr Comp Physiol. 2011;301(3):R676-81.

4. Dumesic DA, Lobo RA. Cancer risk and PCOS. Steroids. 2013;78(8):782-5.

5. González F, Sia CL, Bearson DM, Blair HE. Hyperandrogenism induces a proinflammatory TNFα response to glucose ingestion in a receptor-dependent fashion. J Clin Endocrinol Metab. 2014;99(5):E848-54.

6. Zhang J, Bao Y, Zhou X, Zheng L. Polycystic ovary syndrome and mitochondrial dysfunction. Reprod Biol Endocrinol. 2019;17(1):67.

7. Mohammadi M. Oxidative stress and polycystic ovary syndrome: a brief review. Int J Prev Med. 2019;10:86.

8. Choi JJ, Yoo SA, Park SJ, Kang YJ, Kim WU, Oh IH, et al. Mesenchymal stem cells overexpressing interleukin-10 attenuate collagen-induced arthritis in mice. Clin Exp Immunol. 2008;153(2):269-76.

9. Genc B, Bozan HR, Genc S, Genc K. Stem cell therapy for multiple sclerosis. Adv Exp Med Biol. 2019;1084:145-74.

10. Chen S, Tang K, Hu P, Tan S, Yang S, Yang C, et al. Atractylenolide III alleviates the apoptosis through inhibition of autophagy by the mTOR-dependent pathway in alveolar macrophages of human silicosis. Mol Cell Biochem. 2021;476(2):809-18.

11. Lin MJ, Chen HW, Liu PH, Cheng WJ, Kuo SL, Kao MC. The prescription patterns of traditional Chinese medicine for women with polycystic ovary syndrome in Taiwan: a nationwide population-based study. Medicine (Baltimore). 2019;98(24):e15890.

12. Hu W, Xie N, Zhu H, Jiang Y, Ding S, Ye S, et al. The effective compounds and mechanisms of Cang-Fu-Dao-Tan Formula in treating polycystic ovary syndrome based on UPLC/Q-TOF-MS/MS, network pharmacology and molecular experiments. J Pharm Biomed Anal. 2024;239:115867.

13. Lee JC, Pak SC, Lee SH, Lim SC, Bai YH, Jin CS, et al. The effect of herbal medicine on nerve growth factor in estradiol valerate-induced polycystic ovaries in rats. Am J Chin Med. 2003;31(6):885-95.

14. Li MF, Zhou XM, Li XL. The effect of berberine on polycystic ovary syndrome patients with insulin resistance (PCOS-IR): a meta-analysis and systematic review. Evid Based Complement Alternat Med. 2018;2018:2532935.

15. Chugh RM, Park HS, El Andaloussi A, Elsharoud A, Esfandyari S, Ulin M, et al. Mesenchymal stem cell therapy ameliorates metabolic dysfunction and restores fertility in a PCOS mouse model through interleukin-10. Stem Cell Res Ther. 2021;12(1):388.

16. Kauffman AS, Thackray VG, Ryan GE, Tolson KP, Glidewell-Kenney CA, Semaan SJ, et al. A novel letrozole model recapitulates both the reproductive and metabolic phenotypes of polycystic ovary syndrome in female mice. Biol Reprod. 2015;93(3):69.

17. Nouri F, Nematollahi-Mahani SN, Sharifi AM. Preconditioning of mesenchymal stem cells with non-toxic concentration of hydrogen peroxide against oxidative stress induced cell death: the role of hypoxia-inducible factor-1. Adv Pharm Bull. 2019;9(1):76-83.

18. Ott M, Gogvadze V, Orrenius S, Zhivotovsky B. Mitochondria, oxidative stress and cell death. Apoptosis. 2007;12(5):913-22.

19. Lee C, Nam JS, Lee CG, Park M, Yoo CM, Rhee HW, et al. Analysing the mechanism of mitochondrial oxidation-induced cell death using a multifunctional iridium(III) photosensitiser. Nat Commun. 2021;12(1):26.

20. Bergsbaken T, Fink SL, Cookson BT. Pyroptosis: host cell death and inflammation. Nat Rev Microbiol. 2009;7(2):99-109.

21. Yu P, Zhang X, Liu N, Tang L, Peng C, Chen X. Pyroptosis: mechanisms and diseases. Signal Transduct Target Ther. 2021;6(1):128.

22. Li Y, Jiang Q. Uncoupled pyroptosis and IL-1β secretion downstream of inflammasome signaling. Front Immunol. 2023;14:1128358.

23. Khansari N, Shakiba Y, Mahmoudi M. Chronic inflammation and oxidative stress as a major cause of age-related diseases and cancer. Recent Pat Inflamm Allergy Drug Discov. 2009;3(1):73-80.

24. Uchmanowicz I. Oxidative stress, frailty and cardiovascular diseases: current evidence. Adv Exp Med Biol. 2020;1216:65-77.

25. Atashi F, Modarressi A, Pepper MS. The role of reactive oxygen species in mesenchymal stem cell adipogenic and osteogenic differentiation: a review. Stem Cells Dev. 2015;24(10):1150-63.

26. Navaratnarajah T, Bellmann M, Seibt A, Anand R, Degistirici Ö, Meisel R, et al. Mesenchymal stem cells improve redox homeostasis and mitochondrial respiration in fibroblast cell lines with pathogenic MT-ND3 and MT-ND6 variants. Stem Cell Res Ther. 2022;13(1):256.

27. Irato P, Santovito G. Enzymatic and non-enzymatic molecules with antioxidant function. Antioxidants (Basel). 2021;10(4):579.

28. Jeeva JS, Sunitha J, Ananthalakshmi R, Rajkumari S, Ramesh M, Krishnan R. Enzymatic antioxidants and its role in oral diseases. J Pharm Bioallied Sci. 2015;7 Suppl 2:S331-3.

29. Fang Z, Kim HG, Huang M, Chowdhury K, Li MO, Liangpunsakul S, et al. Sestrin proteins protect against lipotoxicity-induced oxidative stress in the liver via suppression of c-Jun N-terminal kinases. Cell Mol Gastroenterol Hepatol. 2021;12(3):921-42.

30. Semba T, Sammons R, Wang X, Xie X, Dalby KN, Ueno NT. JNK signaling in stem cell self-renewal and differentiation. Int J Mol Sci. 2020;21(7):2613.

31. Gu H, Huang Z, Yin X, Zhang J, Gong L, Chen J, et al. Role of c-Jun N-terminal kinase in the osteogenic and adipogenic differentiation of human adipose-derived mesenchymal stem cells. Exp Cell Res. 2015;339(1):112-21.

32. Serna R, Ramrakhiani A, Hernandez JC, Chen CL, Nakagawa C, Machida T, et al. c-JUN inhibits mTORC2 and glucose uptake to promote self-renewal and obesity. iScience. 2022;25(6):104325.